Contemporary Engineering Sciences, Vol. 11, 2018, no. 53, 2641 - 2650
HIKARI Ltd, www.m-hikari.com
https://doi.org/10.12988/ces.2018.86273

Development of Non-Conservative Mechanical Models Applied to the Low Energy Impact Phenomenon

Milton F. Coba Salcedo[1], Carlos Acevedo Peñaloza [2] and Javier Navas Lopez[3]

[1] Materials Engineering and Manufacturing Technology Research Group – IMTEF, Universidad del Atlántico, Carrera 30 Número 8 – 49
Puerto Colombia – Colombia

[2] Mechanical Engineering Department, Faculty of Engineering
Universidad Francisco de Paula Santander, Colombia

[3] Mechanical Engineering Department, Catalan Company of Elevators, Spain

Abstract

Non-conservative mechanical models are developed to be applied to the low energy impact phenomenon. The analytical description of the proposed models is made and the numerical solution of the system of differential equations is proposed. The impact of materials is undoubtedly the object of research, due to the dynamic condition inherent in the bodies that interact in our universe. That is why we have standardized methodologies for its study, such as Izod and Charpy impact techniques, among others. However, this work places special emphasis on the method of plate bending, which, due to its geometric configuration, interprets real impact situations to which some bodies are subjected, in addition to the low energy technique in which the energy available in the impactor is less than that absorbed in the breaking process, makes it possible to obtain information on the material in the elastic, plastic, initiation and crack propagation range.

Keywords: impact, Charpy, Plastics, non conservative models

1. Introduction

The evolution of the knowledge of physical phenomena has found in modelling a strong tool to interpret their real behavior [1], in this sense, the present work intends to apply this tool to the low energy impact phenomenon, using non-conservative models. The use of non-conservative models is based on the fact that there are considerable energy losses, which explain why conservative models, although they give an idea of the phenomenon, are not the best results [2]. Fracture processes in plastic materials are influenced by their properties. Polymers do not have the structural regularity of other materials such as ceramics and metals, although some polymers have a certain crystalline structure, the presence of macromolecules makes their accommodation and cohesion strength different from that of other materials, thus influencing their mechanical properties [3]. That is to say, an essential characteristic of polymers is that they are formed by long chains of macromolecules that in turn entangle each other, and it can be observed that their structure, apparently a solid, is in fact more similar to that of liquids. This is why it is considered to be a new state of matter between solids and liquids, called the visco-elastic state. Because it is a very elastic solid or a very viscous liquid [4]. Due to the viscoelastic state of the polymers, the deformation mechanisms depend on time, this exclusive property of the polymers is of special relevance for their study and application, since in the search for relating the structure of the materials with their mechanical behaviour, reliable methods must be established to characterize the response of the materials in low, medium and high speed conditions [5]. Within these ranges, materials subjected to impact play an important role and require further research, along with the use of additional techniques and equipment to complement and improve existing impact tests. The impact techniques used to evaluate the impact behaviour of plastic materials have evolved ostensibly from sophisticated equipment and from classical techniques to the development of the theory of fracture mechanics [6]. References of work based on these advances can be found in studies carried out on impact techniques, fracture mechanics, and characterization in quasi-static or high-speed conditions of stressing polymer materials (natural or modified). In the investigations of Sánchez-M [7], Jiménez-O [8] or Gámez-J [9].

2. Methodology

2.1. Model development. Bending model non-conservative parallel-series indentation

It is proposed to develop a model that interprets together the indentation and flexion that a body experiences when subjected to impact. In this sense, the following phases of the new model are proposed: Indentation phase. A series indentation model is developed, consisting of the arrangement of a non-linear spring and a linear damper in series (see Figure 1a), which was studied and tested in multiple indentation tests. Bending phase, a parallel arrangement is proposed, which consists of the arrangement of a linear spring and a linear damper in parallel (see figure 1b). In such a way that the configuration obtained is a new bending/indentation model with a non-conservative parallel parallel series, which consists of a mass element (m), 2 linear dampers (one with *Ci* indentation and the other with *Cf* bending) and two elastic elements (one linear for *Kf* bending and the other non-linear due to *Ki* indentation) see figure 1c.

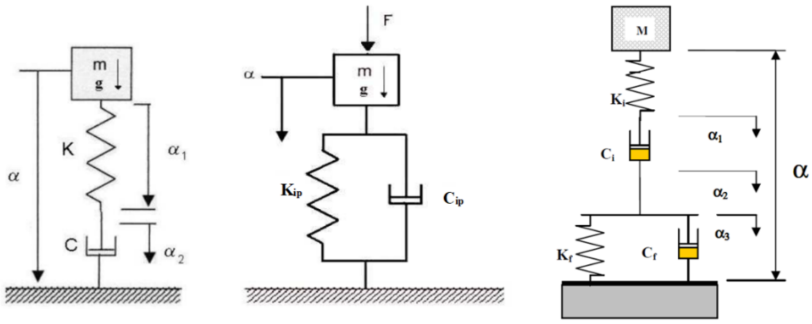

a) Non-conservative serial Indentation Model

b) Non-conservative parallel bending model

c) Non-conservative bending/indentation model for parallel series

Figure 1. Non-conservative bending/indentation model for parallel series

The equations that govern the system in Figure 1 are:

$$F_m = m * \ddot{\alpha} + mg \tag{1}$$

$$Fc_i = C_i * \alpha * c_i \tag{2}$$

$$Fc_f = C_f * \alpha * c_f \tag{3}$$

$$F_{Kf} = K_f * \alpha_{Kf} \tag{4}$$

$$F_{Ki} = K_i * \alpha_{Ki} \tag{5}$$

The model in figure 1c represents the collision of the low energy impactor-probe system, where:

m, mass of the impactor.
K, the constant of the springs.
C, damping coefficient.
Subscript *i* is used for indentation and *f* for bending.
The *Ki* spring is non-linear (Hertzian).

As it is a series-parallel model, the applied force must be analyzed in each element, while the total displacement is the sum of the individual ones, taking into account that the displacement of K_f and C_f are the same. From the model it follows that the constants K_f and K_i, according to the theory of simply supported discs [11, 12], are expressed as:

$$K_f = \frac{16\pi(1+v)*D}{(3+v)*r^2} = \frac{4*\pi*E*e^3}{3*(3+v)*(1-v)*r^2} \tag{6}$$

$$K_i = \frac{4*\sqrt{R}}{3*\pi*(K_1+K_2)} = \frac{4*\sqrt{R}}{3*\pi}\left(\frac{1-v_1^2}{E_1} + \frac{1-v_2^2}{E_2}\right)^{-1} \tag{7}$$

The constant C_f is defined as:

$$C_f = \frac{2*\sqrt{K_m}}{\sqrt{1+\left(\frac{\pi}{ln\varepsilon}\right)^2}} \tag{8}$$

In the case of C_i it is a factor to be adjusted for the whole solution. Displacements are defined as:

$$\alpha = \alpha_1 + \alpha_2 + \alpha_3 \tag{9}$$

Where α is the total displacement of the system as well as the mass element.

- $\alpha_{Ki} = \alpha_1$, corresponds to the elastic part of the indentation.
- $\alpha_{Ci} = \alpha_2$, describing the non-elastic deformation of the indentation.
- $\alpha_{Kf} = \alpha_{Cf} = \alpha_3$, describes the displacement due to bending of both elastic and non-elastic parts.

When constructing the system of differential equations that describes the behavior of the system we have to:

$$m * \ddot{\alpha} = K_i * \alpha_1^{3/2} \tag{10}$$

$$K_i * \alpha_1^{3/2} = C_i * \alpha_2 \tag{11}$$

$$K_i * \alpha_1^{3/2} = K_F * \alpha_3 + C_F * \alpha_3 \tag{12}$$

The term of the gravitational effect has been disregarded. The appearance of the non-linear term corresponding to Hertz's law prevents us from finding an analytical solution that satisfies the system, and that is why the numerical method of Runge-Kutta of 4th order has been used to solve it.

3. Results and discussion

3.1. Numerical solution

Since in the development of the equations we observe that a spring has a non-linear behavior, the differential equation proposed lacks a solution that can be represented by an analytical function. However, it is possible to find a numerical function that is a solution to this problem. As this is an ordinary differential equation, it is possible to use numerical methods for its resolution. Numerical methods are based on algorithms, which take the initial conditions to perform the calculations iteratively, the convenience of the method determines it, the required accuracy and the breadth of the study range. For this case, the study interval is

relatively long, so the Euler and Euler-Gauss methods are not optimal because they do not provide valid solutions far from the vicinity of the starting point. However, the 4th order Runge Kutta method, despite the large number of calculations required, allows generating a numerical function that is the solution of an ordinary differential equation over a longer interval.
The Runge Kutta method is based on the calculation of slopes between a known point and the one you want to know. It makes use of the first terms of Taylor's series. This makes it possible to program it and calculate the solution with a high density of points. In this case, since the differential equation has more than one variable and its respective derivatives, it is necessary to express the model as a system of ordinary equations related to each other that allows us to calculate the different variables. Once the numerical method to be used has been established, in order to find the function that satisfies the system of equations, it is necessary to express this system so that we can program the method. From equation (9) it follows that:

$$\alpha_1 = \alpha - \alpha_2 - \alpha_3 \tag{13}$$

From equation (13) it is necessary to:

$$\alpha_2 = \frac{K_i}{C_i} * \alpha_1^{3/2} \tag{14}$$

Replacing (13) in equation (14) has:

$$\alpha_2 = \frac{K_i}{C_i} * (\alpha - \alpha_2 - \alpha_3)^{3/2} \tag{15}$$

From equation (10) and (11) it is necessary to:

$$\ddot{\alpha} = -\frac{C_i}{m} * \alpha_2 \tag{16}$$

Replacing equation (15) with (16) gives:

$$\alpha = -\frac{C_i}{m} * \left(\frac{K_i}{C_i} * (\alpha - \alpha_2 - \alpha_3)^{3/2}\right)$$

Simplifying

$$\ddot{\alpha} = -\left(\frac{K_i}{m} * (\alpha - \alpha_2 - \alpha_3)^{3/2}\right) \tag{17}$$

Starting from equation (12) it is necessary to:

$$\alpha_3 = \frac{1}{C_F} * \left(K_i * \alpha_1^{3/2} - K_F * \alpha_3\right) \tag{18}$$

And by replacing equation (13) in (19) it is necessary to:

$$\alpha_3 = \frac{1}{C_F} * (K_i * (\alpha - \alpha_2 - \alpha_3)^{\frac{3}{2}} - K_F * \alpha_3) \tag{19}$$

Expressions (15), (17), and (19) allow you to build the function system required by the Runge Kutta method. However, the presence of 4 derivatives (3 explicit and a fourth that does not appear) makes it necessary to have a fourth equation, so, in addition to the three previous equations, we define a fourth function that allows us to calculate all the variables that appear.

$$\alpha = \frac{\partial \alpha}{\partial t} \tag{20}$$

In this way, the set of functions is expressed as:

$$f_i = \frac{K_i}{C_i} * (\alpha - \alpha_2 - \alpha_3)^{3/2} \tag{21}$$

$$f_2 = -\left(\frac{K_i}{m} * (\alpha - \alpha_2 - \alpha_3)^{3/2}\right) \tag{22}$$

$$f_3 = \frac{1}{C_F} * \left(K_i * (\alpha - \alpha_2 - \alpha_3)^{3/2} - K_F * \alpha_3\right) \tag{23}$$

$$f_4 = \alpha = \frac{\partial \alpha}{\partial t} \tag{24}$$

With this system of equations, the algorithm was developed and programmed in Excel for the ease with which this program can handle data tables and dynamic calculation, as well as for its convenience in visualizing the different variables and results. In its programming the intervals of 1 or 2 µs are used between each calculated point. These will correspond to the same time interval as the data acquisition equipment used in the experiments. For the operation of the algorithm the initial conditions are:

- Impact velocity ($\alpha_{t=0} = v_0$)
- Non-elastic strain rate (damping element); ($\alpha_{\ 2,t=0} = 0$)
- The acceleration of the mass element ($\ddot{\alpha} = 0$)

The parameters of the model are the mass of the impactor (m) and the constants K (related to the elastic part) and C (related to the loss of energy and therefore to the restitution coefficient). These two parameters can be manually varied to adjust the model to the experimental values.

3.2. Non-conservative series-parallel bending-indentation model considering gravitational effects

In this model, the collision of the impactor-probe system at low energy is represented by the arrangement of figure 2, the model considers the mass of the specimen (mp). Where:

m, mass of the impactor.
mp, mass of the test tube.
K, the constant of the springs.
C, damping coefficient.
Subscript *i* is used for indentation and *f* for bending.
The *Ki* spring is non-linear (Hertzian).

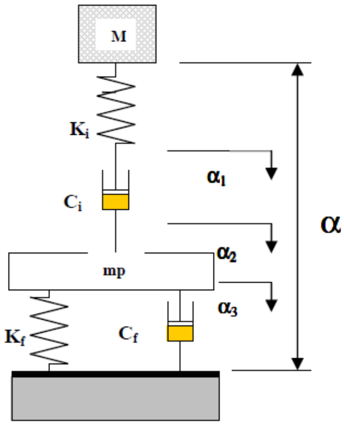

Figure 2. Non-conservative parallel series bending/indentation model with effective specimen mass.

The equations governing the system in Figure 2 are:

$$F_m = m * \ddot{\alpha} + m * g \tag{25}$$

$$F_{Ci} = C_i * \alpha_{Ci} \tag{26}$$

$$F_{Cf} = C_f * \alpha * c_f \tag{27}$$

$$F_{Kf} = K_f * \alpha_{Kf} \tag{28}$$

$$F_{Ki} = K_i * \alpha_{Ki} \tag{29}$$

The constants K_f and K_i are defined as
:

$$K_F = \frac{16\pi(1+v)D}{(3+v)r^2} = \frac{4\pi E e^3}{3(3+v)(1-v)r^2} \tag{30}$$

$$K_i = \frac{4\sqrt{R}}{3\pi(K_1+K_2)} = \frac{4\sqrt{R}}{3\pi}\left(\frac{1-v_1^2}{E_1} + \frac{1-v_2^2}{E_2}\right)^{-1} \tag{31}$$

The constant C_f is defined as:

$$C_f = \frac{2\sqrt{K_m}}{\sqrt{1+\left(\frac{\pi}{In\varepsilon}\right)^2}} \tag{32}$$

In the case of C_i is a factor that needs to be adjusted so that overall the solution. Displacements are defined as:

$$\alpha = \alpha_1 + \alpha_2 + \alpha_3 \tag{33}$$

Where α is the total displacement of the system as well as the mass element. When constructing the system of differential equations that describes the behavior of this system we have to:

- $\alpha_{Ki} = \alpha_1$, corresponding to the elastic part of the indentation.
- $\alpha_{Ci} = \alpha_2$, describing the non-elastic deformation of the indentation.
- $\alpha_{KF} = \alpha_{Cf} = \alpha_3$, describes the displacement due to bending of both elastic and non-elastic parts.

When constructing the system of differential equations that describes the behavior of this system we have to:

$$m * \ddot{\alpha} + m * g = K_\iota * \alpha_1^{3/2} \tag{34}$$

$$K_i * \alpha_1^{3/2} = C_i * \alpha_2 \tag{35}$$

$$m * p * \ddot{\alpha} + m * p * g = K_i * \alpha_1 - C_F * \alpha_3 - K_F * \alpha_3 \tag{36}$$

The appearance of the non-linear term corresponding to Hertz's law prevents us from finding an analytical solution that satisfies the system, and that is why the numerical method of Runge-Kutta of 4th order has been used to solve it. From equation 33 it follows that:

$$\alpha_1 = \alpha - \alpha_2 - \alpha_3 \tag{37}$$

From equation 35 it is necessary to:

$$\alpha_2 = \frac{K_i}{C_I} * \alpha_1^{3/2} \tag{38}$$

Replacing equation (36) with (37) gives:

$$\alpha_2 = \frac{K_i}{C_i} * (\alpha - \alpha_2 - \alpha_3)^{3/2} \tag{39}$$

By replacing equation (35) in (34) you have:

$$\ddot{\alpha} = -\frac{C_i}{m} * \alpha_2 - g \tag{40}$$

Replacing (36) in equation (38):

$$\ddot{\alpha} = -\frac{C_i}{m} * \left(\frac{K_i}{C_i} * (\alpha - \alpha_2 - \alpha_3)^{\frac{3}{2}}\right) - g \tag{41}$$

Simplifying:

$$\ddot{\alpha} = -\left(\frac{K_i}{m} * (\alpha - \alpha_2 - \alpha_3)^{\frac{3}{2}}\right) - g \tag{42}$$

Starting from equation (36) it is necessary to:

$$\ddot{\alpha} = -\frac{K_I}{mp} * (\alpha_1)^{\frac{3}{2}} - \frac{K_F}{mp} * \alpha_3 - \frac{C_F}{mp} * \alpha_3 - g \tag{43}$$

Replacing equation (36) with (42) gives:

$$\ddot{\alpha}_3 = -\frac{K_I}{mp} * (\alpha - \alpha_2 - \alpha_3)^{\frac{3}{2}} - \frac{K_F}{mp} * \alpha_3 - \frac{C_F}{mp} \alpha_3 - g \tag{44}$$

Expressions (38), (41) and (43) allow you to build the function system required by the Runge-Kutta method. However, the presence of 4 derivatives (3 explicit and a fourth that does not appear) makes it necessary to have a fourth equation, so in addition to the three previous equations, a 4th function was defined to calculate all the variables that appear.

$$\dot{\alpha} = \frac{\partial \alpha}{\partial t} \quad (45)$$

In this way, the set of functions is defined as:

$$f_1 = \frac{K_i}{C_i} * (\alpha - \alpha_2 - \alpha_3)^{3/2} \quad (46)$$

$$f_2 = -\left(\frac{K_i}{m}(\alpha - \alpha_2 - \alpha_3)^{\frac{3}{2}}\right) - g \quad (47)$$

$$f_3 = -\left(\frac{K_I}{mp} * (\alpha - \alpha_2 - \alpha_3)^{\frac{3}{2}}\right) - \frac{K_F}{mp} * \alpha_3 - \frac{C_F}{mp} * \alpha_3 - g \quad (48)$$

$$f_4 = \alpha = \frac{\partial \alpha}{\partial t} \quad (49)$$

With this system of equations an algorithm was developed and programmed.

- Speed of impact $(\alpha_{t=0,} = v_0)$
- Non-elastic strain rate (shock-absorbing element); $\left(\alpha_{2,t=0} = 0\right)$
- The acceleration of the mass element $(\ddot{\alpha} = 0)$
- The acceleration of the mass element $(\ddot{\alpha}_3 = 0)$

The parameters of the model are the mass of the impactor (*m*), the mass of the test piece (*mp*) and the constants *K* (related to the elastic part) and *C* (related to the loss of energy and therefore to the coefficient of restitution). These two parameters can be manually varied to fit the model to the experimental values.

4. Conclusions

The application of the bending and indentation models with and without mass allows distinguishing at what value of the energy or the maximum force the beginning of the damage in the specimen takes place. The models allow us to discriminate dynamic phenomena due to the impact of the energy absorbed and recovered by the material, even allowing us to differentiate the behavior of two materials that may consume the same energy or present similarity in the force-time curve. The parallel series model with mass, in addition to reproducing the quasi-sinusoidal shape of the experimentally obtained curves, also reproduces the undulations present in the tests performed, which are motivated by inertial forces due to the effective mass of the test tube.

References

[1] M. A. Macaulay, *Introduction to Impact Engineering*, 1st Edition, Springer New York, Editorial Chapman and Hall, 1987.

https://doi.org/10.1007/978-94-009-3159-6

[2] W. Goldsmith, *Impact: The Physical Theory and Behaviour of Colliding Solids*, London: Edward Arnold Ltd., 1960.

[3] S. Turner, *Mechanical Testing of Plastics*, 2nd Edition, The Plastics and Rubber Institute, Londres, 1983.

[4] T. A. Oswald and G. Menges, eds., *Material Science of Polymers for Engineers*, 2nd Edition, Hanser, Munich, 2003.

[5] J. G. Williams, *Fracture Mechanics of Polymers*, 1st Edition, Ellis Horwood Series in Engineering Science, Chichester, 1994.

[6] A. B. Martínez, Técnicas de impacto de materiales plásticos y compuestos, 1ª.

[7] Edición, Publicaciones Universidad Politécnica de Cataluña, Barcelona, 1988.

[8] Sánchez-Soto M, Comportamiento mecánico y fractura de mezclas de poliestireno y microesferas de vidrio, Tesis CCP, UPC Terrassa, 2000.

[9] O. A. Jiménez Arévalo, *Comportamiento a la Fractura de Composites Con Matriz de Poliestireno*, Diss., Universidad Politécnica de Cataluña, Terrassa, 2002.

[10] J. Gámez Pérez, *Relación Estructura-Propiedad En Placas Y Láminas De Polipropileno Y Copolímeros En Bloque Etileno-Propileno Obtenidas Por Diferentes Procesos De Transformación*, Diss., Universitat Politècnica de Catalunya CCP, UPC Terrassa, 2006.

[11] Javier Antonio Navas López, Estudio, *Evaluación Y Modelado Del Comportamiento De Indentación Y Flexión-Indentación A Impacto De Baja Energía De Materiales Termoplásticos*. Diss., Universidad Politecnica de Cataluña. Barcelona, 2008.

[12] R .J. Roark, *Formulas for Stress and Strain*, Mc Graw Hill, New York, 1954.

[13] W. C. Young, *Roark's Formulas for Stress and Strain*. 6 Edition, Mc Graw Hill, New York, 1989.

Received: June 23, 2018; Published: July 18, 2018